Review Article/Telecommunications Engineering

http://doi.org/10.15446/ing.investig.115406

Calculating the Changes in the User Terminal Figure of Merit (G/T) as a Function of Link Conditions: A Review

Cálculo de los cambios en la figura de mérito de las estaciones de usuario (G/T) en función de las condiciones del enlace: una revisión

Luis EMILIANI[1]

ABSTRACT

Activities such as the design and optimization of satellite constellations for telecommunications, communication solutions engineering, or GEO/non-GEO satellite inter-system coexistence applications benefit from methods to compute changes in Earth station equivalent noise temperature, a product of the dynamic nature of link geometry and the propagation channel. This paper addresses said requirement. Starting with a review of the user terminal G/T and Earth station noise temperature, methods are developed to compute the change in noise temperature introduced by varying elevation angle and propagation channel conditions. These methods are useful for engineering analyses when the noise contributions from each component of the Earth station receive chain are not known, especially considering the increased impact of clouds and gasses on GEO and non-GEO links operating in frequencies of the Q, E, and W bands. Examples of use and benefits are provided, as well as considerations on the applicability and validity of the methods.

Keywords: satellite communications, Earth stations, figure of merit, antenna temperature, sky brightness, system noise temperature.

ABSTRACT

Actividades como el diseño y la optimización de constelaciones de satélites para telecomunicaciones, la ingeniería de soluciones de comunicación o las aplicaciones de coexistencia intersistémica entre satélites GEO y no GEO se benefician de métodos para calcular los cambios en la temperatura equivalente de ruido de la estación terrena, un producto de la naturaleza dinámica de la geometría del enlace y del canal de propagación. Este artículo aborda dicho requerimiento. A partir de una revisión de la G/T del terminal de usuario y de la temperatura de ruido de la estación terrena, se desarrollan métodos para calcular el cambio en la temperatura de ruido introducido por la variación del ángulo de elevación y de las condiciones del canal de propagación. Estos métodos son útiles para los análisis de ingeniería cuando no se conocen las contribuciones de ruido de cada componente de la cadena de recepción de la estación terrena, especialmente considerando el mayor impacto de las nubes y los gases en enlaces GEO y no GEO que operan en las bandas Q, E y W. Se presentan ejemplos de uso y beneficios, así como consideraciones sobre la aplicabilidad y validez de los métodos.

Palabras clave: comunicaciones satelitales, estación terrena, figura de mérito, temperatura de ruido de antena, temperatura de ruido

Received: June 28th, 2024
Accepted: November 19th, 2025

Introduction

The accurate characterization of the noise temperature at the ground station of a satellite communication system (henceforth known as the *Earth station*) is fundamental in the analysis of satellite links [1, 2]. Earth station noise temperature plays a critical role in calculating the carrier-to-noise ratio (C/N) of the space-to-Earth link, and, in the context of inter-system coordination, it is used to analyze the interference-to-noise ratio (I/N) experienced at a victim Earth station.

Where possible, the system noise temperature T_{sys} should be computed while considering the path propagation loss (in clear weather or rain conditions) and its effect on antenna noise temperature, which requires an Earth station receive chain model and full knowledge of its components (e.g., radome and feeder losses, low-noise block down-converter, or LNB, and receiver noise temperatures).

However, there are scenarios where not all the elements required for calculating the Earth station noise temperature are available, which necessitates models that help to determine the system noise temperature both in clear weather ($T_{sys,\ C.W.}$) and under degraded conditions ($T_{sys,\ rain}$), including the effects of elevation angle variations, all in the presence of limited technical data. Such cases arise in the preliminary design of geostationary (GEO) and non-geostationary (non-GEO) satellite communication systems, especially during the procedures associated with the preparation of regulatory filings for satellite networks, or in scenarios involving inter-service spectrum sharing, such as [3, 4], which often use an aggregate system noise temperature value without reference to a receive chain model or detailing the contribution of each element of the chain. A proper understanding of the reasons for the expected changes in system noise temperature is of particular importance considering the frequency allocations

[1] Electronics engineer, Universidad Pontificia Bolivariana, Colombia. Master in Engineering, Universidad Pontificia Bolivariana, Colombia. Affiliation: Senior manager, Fleet Advancement, SES, Luxembourg. Email: Luis.emiliani@gmail.com

to the space-to-Earth (s-E) path in higher frequency bands such as Q (37.5-43.5 GHz), E (71-76GHz), and W (123-130GHz) for GEO and non-GEO satellite communications system [5], where the attenuation (and associated radio noise) due to gas and clouds under clear-sky conditions should not be ignored.

Considering that the prevailing approach in the literature is to start from complete knowledge of the receive chain, with access to all the information required for system temperature calculations (*i.e.*, $T_{ant}, T_{RAD}, T_{feed}, T_{LNB}$), the purpose of this paper is to review the simplified methods used when the only available information is an aggregate value of T_{sys}. These methods aim to help communication systems engineers carry out activities related to solutions engineering, constellation capacity analysis, system design, and critical regulatory procedures such as satellite network filings and inter-system co-existence. The minimum amount of data required is either the value of G/T (which can be read from a manufacturer datasheet and from which a T_{sys} value could be derived) or b) the total noise temperature. To this effect, a typical reference Earth station noise temperature model is used to develop expressions aimed at computing noise temperature changes under various conditions, which can be used to analyze wanted and interfering links, relying on statistical methods for propagation impairment calculations.

The paper is structured as follows. First, the concepts of *figure of merit* (G/T) and *Earth station noise temperature* are revisited. Subsequently, the methodology used to develop the two contributions of this paper is presented, followed by the derivation of each model and a study of potential avenues to simplify the resulting equations. After developing the two methods, numerical applications are provided as an illustration. Finally, the paper provides some conclusions and opportunities for further developing the proposed models.

The figure of merit of an Earth station: definition and background

The quality of the received signal in a satellite communication system, quantified by the carrier-to-noise ratio, is largely dictated by the characteristics of the receiving system. The main parameter used to characterize the receive capability of a satellite Earth station is the figure of merit, or *G/T*, mathematically expressed in linear units as follows [2]:

$$\left[\frac{G}{T}\right]_{\text{dB}} = 10 \cdot \log_{10}\left(\frac{g}{T_{\text{sys}}}\right) \tag{1}$$

where g is the composite receive system gain; and T_{sys}, expressed in Kelvins, is the receive system's total noise temperature. $[\cdot]$ indicates that the value in the brackets is in decibels. As previously mentioned, G/T directly influences the receive carrier-to-noise power density ratio, $\frac{C}{N_0}$, which is computed as follows [1]:

$$\frac{C}{N_0} = Transmitter\ EIRP \cdot \frac{1}{l} \cdot \frac{G}{T} \cdot \frac{1}{k}, \tag{2}$$

with k being the Boltzmann constant ($1.380649 * 10^{-23}\ J/K$), and l the total path loss.

Establishing a reference model for T_{sys}, the Earth station equivalent noise temperature

In Eq. (1), the system gain g and the system noise temperature T_{sys} are computed up to a *reference plane* in the receive chain, usually placed at the input of the first amplifying stage of the Earth station, the low noise amplifier (LNB). The accumulated gain up to the reference plane includes the contribution of the antenna and any losses introduced by passive elements in the signal path.

The second component required to calculate the G/T is the system noise temperature. To illustrate the concept of *equivalent noise temperature*, Fig. 1 provides a generic representation of a compact satellite user terminal pertinent to the scenarios mentioned in the introduction. The figure presents the elements used to construct the reference system noise model: the antenna subsystem, including a radome structure; a passive network connecting the antenna to the LNB; and the LNB itself.

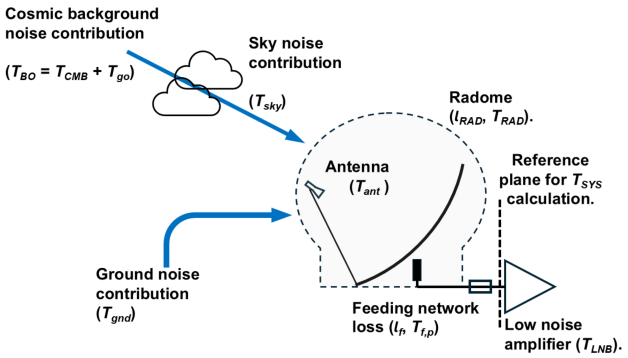

Figure 1. Reference user terminal diagram, reference plane, and noise contributions
Source: Author

Considering that, in satellite communication systems, the level of the received signals could be in the order of picowatts and comparable in magnitude to the system's thermal noise power levels, the treatment of noise in general has been the subject of various research works, as well as the contribution of the various elements in a receive chain to the total system noise. Among the most complete works on the topic of satellite ground station system noise are those conducted in the context of the deep space missions of the National Aeronautics and Space Administration (NASA) [6], which include system configuration, total system noise [7, 8], and atmosphere-induced noise [9]. Furthermore, on the topic of antenna noise temperature, a detailed background can be found in the works associated to the development of the Square-Kilometre Array (SKO) [10] and the next-generation Very Large Array (ngVLA) radio telescopes [11, 12, 13].

In this work, the system temperature model is constructed while applying the principles described in [8]. Recalling that the noise temperature of a passive network regarding its output is $T = T_p \cdot (1 - l_f^{-1})$, the total system noise is expressed as follows:

$$T_{\text{sys}} = \frac{T_{\text{ant}}}{l_f} + T_{\text{f,p}} \cdot (1 - l_f^{-1}) + T_{\text{LNB}}, \tag{3}$$

where:

- T_{ant} (K) is the antenna's noise temperature
- l_f, with a magnitude greater than 1, is the feeding network loss in linear units, *i.e.*, $10^{(0.1 \cdot L)}$
- $T_{\text{f,p}}$ (K) is the feeding network's physical temperature
- T_{LNB} (K) is the equivalent noise temperature of the LNB

In Eq. (3), the feeding network consists of a passive network connecting the antenna flange (usually a reflector antenna) to the LNB. In very small user terminals, this passive network may be a single waveguide, but, in larger Earth stations, the passive network may include waveguide switches – especially when redundant LNB systems are installed– or filters designed to reject unwanted portions of the spectrum for interference reduction (*e.g.*, 5G interference mitigation filters widely used in C-band Earth stations). In this model, we lump the losses of any passive elements between the antenna flange and the LNB into an equivalent loss value.

Origin of the dependence of T_{sys} on the elevation angle and propagation channel conditions

The model presented in Eq. (3) exhibits an Earth station elevation angle dependence that originates from the contribution of the antenna's noise to the total system noise.

The antenna temperature $T_{\text{ant}}(\theta, \phi)$ is the product of $G(\theta, \phi)$, *i.e.*, the antenna radiation pattern, with the distribution of sky and Earth noise over the azimuth and zenith angles (θ, ϕ) in the spherical coordinate system [14]. It is composed of contributions from the sky, including background radiation and atmospheric contributions (gasses, rain, clouds), and emissions from the Earth, *e.g.*, reflected sky emissions captured by the portion of the radiation pattern that intercepts the ground.

In the absence of a radome, under clear weather conditions, the antenna temperature is

$$T_{\text{ant, wo. RAD}} = T_{\text{sky}} + T_{\text{gnd}}. \tag{4}$$

Including the effects of a radome, it is

$$T_{\text{ant}} = \frac{T_{\text{ant,wo. RAD}}}{l_{\text{RAD}}} + T_{\text{RAD, p}} \cdot (1 - l_{\text{RAD}}^{-1}) \tag{5}$$

Decomposing Eq. (5) yields the following:

$$\begin{aligned} T_{\text{ant}} &= \frac{T_{\text{sky}}}{l_{\text{RAD}}} + \frac{T_{\text{gnd}}}{l_{\text{RAD}}} + T_{\text{RAD,p}} \cdot (1 - l_{\text{RAD}}^{-1}) \\ &= \frac{1}{l_{\text{RAD}}} \cdot \left(\frac{T_{\text{Bo}}}{l_{\text{atm, C.W.}}} + T_{\text{atm, C.W.}}\right) + \frac{T_{\text{gnd}}}{l_{\text{RAD}}} \cdots \\ &+ T_{\text{RAD,p}} \cdot (1 - l_{\text{RAD}}^{-1}) \\ &= \frac{T_{\text{Bo}}}{l_{\text{atm, C.W.}} \cdot l_{\text{RAD}}} + \frac{T_{\text{MR}}}{l_{\text{RAD}}} \cdot (1 - l_{\text{atm, C.W.}}^{-1}) + \frac{T_{\text{gnd}}}{l_{\text{RAD}}} \cdots \\ &+ T_{\text{RAD,p}} \cdot (1 - l_{\text{RAD}}^{-1}). \end{aligned} \tag{6}$$

In Eq. (6),

- T_{sky} is the sky's contribution to the antenna noise temperature ($T_{Bo} + T_{\text{atm, C.W.}}$)
- T_{Bo} is the cosmic background's brightness temperature, which can be estimated as a function of frequency [14]:

$$T_{\text{Bo}}(f) = T_{\text{CMB}} + T_{\text{go}} \cdot \left(\frac{f_0}{f}\right)^{\beta} \tag{7}$$

  where T_{CMB}=2.73 K, T_{go}=20 K, f_0=408 MHz, and β=2.75, which, for practical purposes, can be approximated as ≈ 2.73 K
- $T_{\text{atm, C.W.}}$ denotes the sky's brightness, *i.e.*, the equivalent noise temperature of the atmosphere in clear weather, defined as $T_{\text{atm, C.W.}} = T_{\text{MR}} \cdot (1 - l_{\text{atm, C.W.}}^{-1})$
- $l_{\text{atm, C.W.}}$ represents the loss due to gases (O_2 and water vapor) and clouds in clear weather (expressed in linear units)
- T_{MR} is the atmosphere's mean radiating temperature,
- T_{gnd} signifies the ground contribution to the antenna noise temperature
- $T_{\text{RAD, p}}$ denotes the radome physical temperature
- l_{RAD} is the radome loss

All temperatures are in Kelvin, and all losses in linear units are greater than one (>1).

Given the antenna temperature's dependence on the characteristics of the radiation pattern and the path length through the atmosphere, T_{ant} will vary with the antenna elevation angle towards the satellite: firstly, because the slant path length increases with a decreasing elevation angle, thus increasing the magnitude of the contribution from the atmosphere (gas, clouds in clear weather); and secondly, because the ground contribution to the antenna noise will increase with decreasing elevation angles as the portion of the antenna beam solid angle occupied by the ground increases.

Problem context and methodology

Context

As mentioned in the introduction, there are various practical cases in satellite communication systems engineering where it is necessary to conduct link analyses with limited data|for instance, when developing specifications for user terminals, or when optimizing connectivity solutions in a multi-orbit environment. In these cases, only an aggregate value of the target G/T is known or assumed and is held constant across all potential link configurations. Such assumption yields sub-optimal satellite and ground resource consumption results.

Additionally, when working with regulatory information related to satellite networks, such as that contained in ITU-R filings in the context of inter-service sharing, Earth station noise temperature data are not detailed. For Earth stations, the technical information required in a regulatory filing includes the parameter **noise_t**, defined as the total noise

temperature of the receiving system (expressed in Kelvins), referred to the antenna plane, which corresponds to the output of the receiving antenna. No information related to Earth station components or the reference elevation angle is given. Moreover, the data supplied in compliance with Appendix IV of the *Radio Regulations* include the lowest noise temperature value, referred to the antenna plane, applicable across the minimum and maximum elevation angles of operation of the Earth station. The definition of item **C.5.b** reads: "this value shall be indicated for the nominal value of the angle of elevation when the associated transmitting station is onboard a geostationary satellite and, in other cases, for the minimum value of the angle of elevation."

Another regulatory scenario to consider corresponds to the procedures recommended by the ITU-R for the coexistence between GEO and non-GEO networks in the Q/V bands and contained in Resolution 770 of WRC-19 [3] and ITU-R Recommendation no. 2157 [15]. The former presents sets of parameters for reference links using GEO satellites in the Q band (37.5-42.5 GHz, space-to-Earth), to be used in multiple permutations of link configurations that include different user terminal sizes (0.45, 0.6 m), elevation angles (20, 55, 90°), and locations on Earth. All cases share a single value for the user terminal's total noise temperature (340 K), without considering antenna sizes, locations, or elevation angles, aspects that impact the antenna noise temperature.

Thus, the objective of this paper is to develop equations for calculating the changes in the Earth station system noise temperature and, therefore, in the G/T, as a function of changes in the satellite link (due to changes in elevation angle or to increased attenuation), in order to support the analysis of the aforementioned scenarios.

Methodology

The methods developed herein followed a three step process, with the reference system temperature expressed in Eq. (3) as a starting reference point:

1. The reference equation for an increased system noise ΔT_{sys} is formulated as the difference between the reference model and that corresponding to the conditions under analysis (*e.g.*, changes in the elevation angle or increased attenuation).

$$\Delta T_{\text{sys}} = T_{\text{sys, reference}} - T_{\text{sys, condition}} \tag{8}$$

2. The expression for ΔT_{sys} is expanded, and the elements that remain unmodified are eliminated.
3. The resulting expression for ΔT_{sys} is analyzed, identifying avenues for further simplification.

The following sections will apply this process to two link engineering scenarios:

1. Computing the increase in total system noise temperature due to changes in the operating elevation angle under clear weather conditions.
2. Computing the increase in total system noise temperature due to the presence of rain in the propagation path.

Computing the increase in Earth station noise temperature using the elevation angle under clear weather conditions

Changes in the clear weather system temperature with the elevation angle

This subsection applies the general methodology to a case appearing in inter-system coordination and system capacity calculations: the user terminal is characterized by means of a single G/T, without an explicit definition of the noise temperature values for the components of the receive chain at a known elevation angle. This case is typical in the design of satellite constellation concepts and in service performance estimations, which include parametric analyses that involve developing the specifications of the user terminal.

As mentioned in the background section, considering that the antenna temperature depends on the elevation angle, the use of a fixed value can lead to the over- or underestimation of the system capacity or the required spacecraft or ground terminal power resources. This section develops an equation to estimate the changes in the Earth station noise temperature that stem from changes in the elevation angle. This is done through statistical methods for atmospheric attenuation prediction. The proposed model includes the following expression:

$$\Delta T_{\text{sys}}(\theta_1, \theta_2) = T_{\text{sys,C.W}}(\theta_2) - T_{\text{sys,C.W}}(\theta_1) \tag{9}$$

with θ_i being the elevation angles.

The system temperatures for each elevation angle θ_1 and θ_2, as shown in Eq. (9), can be expanded while noting that the noise contributions due to feed loss and the LNB remain constant with changes in the elevation angle, and assuming the ground emissions contribution to vary only slightly (*i.e.*, less than about 5 K) with changes in the elevation angle. The implications of this assumption will be discussed once the model has been fully presented.

Proceeding,

$$\Delta T_{\text{sys}}(\theta_1, \theta_2) = \frac{1}{l_f} \cdot (T_{\text{ant,C.W}}(\theta_2) - T_{\text{ant,C.W}}(\theta_1)) \tag{10}$$

Noting that the background radiation contribution T_{BO} is independent of the elevation angle, the following is considered to further simplify the model:

- The radome loss and its effective noise contribution can be regarded as independent of the elevation angle. This may not be the case for complex radome structures, as it depends on the characteristics of the radome (shape, materials, number of layers, *etc.*).
- The physical temperatures for operating at two different elevation angles can be assumed to be identical under clear weather conditions.

This yields:

$$\Delta T_{\text{sys}}(\theta_1, \theta_2) = \frac{\text{T}_{\text{MR}}}{l_{\text{f}} \cdot l_{\text{RAD}}} \cdot \left(\frac{1}{l_{\text{atm, C.W}}(\theta_1)} - \frac{1}{l_{\text{atm, C.W}}(\theta_2)} \right) \tag{11}$$

In Eq. (11), $\Delta T_{SYS}(\theta_1, \theta_2)$ can be either positive or negative, since the attenuation contribution at one elevation angle could be higher than the contribution at the other.

The attenuation under clear-sky conditions ($l_{\text{atm, C.W}}$) comprises the gas and cloud contributions. For the purposes of link analysis relying on statistical models, it is usually computed at a 50% exceedance value. For both impairments, the atmospheric attenuation (in decibels) is computed according to current ITU-R models [16, 17]:

$$L_{\text{atm,C.W}}(\theta) = L_{\text{atm, C.W}}\ (zenith) \cdot \frac{1}{sin(\theta)}, \tag{12}$$

which, when transformed into linear units, results in

$$l_{\text{atm}_{\text{C.W}}}(\theta) = 10^{\left(0.1 \cdot L_{\text{atm, C.W}}\ (zenith) \cdot \frac{1}{sin(\theta)}\right)}. \tag{13}$$

Eq. (13) can be expressed in terms of the zenith transmission coefficient as defined in ITU-R Recommendation S.733 [18]:

$$\beta_0 = 10^{\left(-0.1 \cdot L_{\text{atm, C.W}}(zenith)\right)} \tag{14}$$

The zenith transmission coefficient is the inverse of the atmospheric loss at the zenith. Its value lies between zero and unity, with a value closer to the latter indicating that the attenuation caused by the atmospheric constituents is lower|and, therefore, the noise contribution.

Substituting Eqs. (13) and (14) into (11) yields the following the expression for $\Delta\ T_{sys}$:

$$\Delta T_{\text{sys}}(\theta_1, \theta_2)\ = \frac{T_{\text{MR}}}{l_f \cdot l_{\text{RAD}}} \cdot \left(\beta_0^{csc(\theta_1)} - \beta_0^{csc(\theta_2)}\right) \tag{15}$$

For convenience, Table 1 provides the values of the zenith transmission coefficient for various frequencies of interest, as computed for two sets of conditions. The first case uses the atmospheric pressure, water vapor content, and temperature from the standard atmospheric profile contained in [19], without including cloud contributions, for a station at sea level (*i.e.*, 0 km altitude). The second case uses the current ITU-R methods for gas and cloud attenuation to compute the median value of the transmission coefficient over a global grid. Computing the transmission coefficient using a standard atmospheric profile is convenient since it is location-independent. However, for frequencies above 22 GHz (excluding the water vapor absorption windows), the computed value will be closer to unity compared to the value considering the water vapor and the cloud liquid water content of the atmosphere. As the frequency increases, the value computed using only gas contributions and a standard atmosphere becomes less reliable.

To complement Table 1, Fig. 2 illustrates the variation in the value of β_0 with geographical location. The coefficient is computed for a 50% probability of exceedance and a frequency of 42 GHz. While the median value over the coordinate grid is close to that computed using the standard atmospheric profile, the differences between tropical and temperate locations become apparent.

Eq. (15) can be used to estimate the change in the equivalent antenna noise temperature with respect to the value at a known elevation angle, which is limited by both the validity of the cosecant scaling assumption and the magnitude of the contribution of ground emissions to the antenna noise temperature. This will be further explained in this paper.

Table 1. Values of β_0 for various frequencies, computed using a standard atmospheric profile for a station at sea level as well as a global grid

Frequency (GHz)	$\beta_{0,\text{STD}}$	$\beta_{0,\text{Median}}$
4	0.991	0.991
11	0.987	0.987
12	0.986	0.986
18	0.969	0.968
22	0.891	0.893
38	0.925	0.919
42.5	0.892	0.885
71	0.695	0.684
73	0.753	0.739

Source: Author

Fig. 3 compares the output of the equation for elevation angle scaling against reported antenna temperature data. The data consist of four pairs of (elevation, T_{ant}) values, per polarization, for a 1.2 m Ka-band terminal [20]. The upper figure presents the values of $T_{ant,\ C.W.}$ as a function of the elevation angle, with dashed lines used to denote the scaled values and solid ones representing the manufacturer data. The relative error, expressed as a percentage, is reported in the lower figure. The overall error is below 5% for elevation angle values above 10°. The scaling equation was applied using the θ_1 = 20 data point as reference and computed at the antenna mid-band frequencies of 20.25 and 20.3 GHz for the linear and circular pol, respectively.

Limitations of the elevation angle scaling model

As indicated in the development of the equation, the proposed scaling model has limitations. The most relevant ones are presented below.

a. **Limitations arising from the ground contribution to the antenna noise.** The development from Eq. (9) to the Model (15) assumed that the changes in the contribution to antenna noise arising from ground emissions could be ignored. The magnitude of the ground contributions to system noise is linked to the characteristics of the radiation pattern of the antenna and, more specifically, to the portion of the pattern that is directed towards the ground. Therefore, these contributions should be more significant in cases where the antenna exhibits high gain towards the ground, which may be the case when operating at grazing angles. Conversely, ground contributions are expected to be small at elevation angles above around 10° or above the null-to-null beamwidth value of the antenna radiation pattern. Failing to model the capture of radiation from the ground imposes a restriction on the validity of this method to elevation angles above 10° (as seen in Fig. 3), where the contribution of ground emissions to antenna noise should be small. Moreover, it must be noted that, for antennas with a small effective aperture, a wide main lobe, and a high sidelobe profile, as well as for phase array antennas with patterns depending on the characteristics of the steering and the orientation

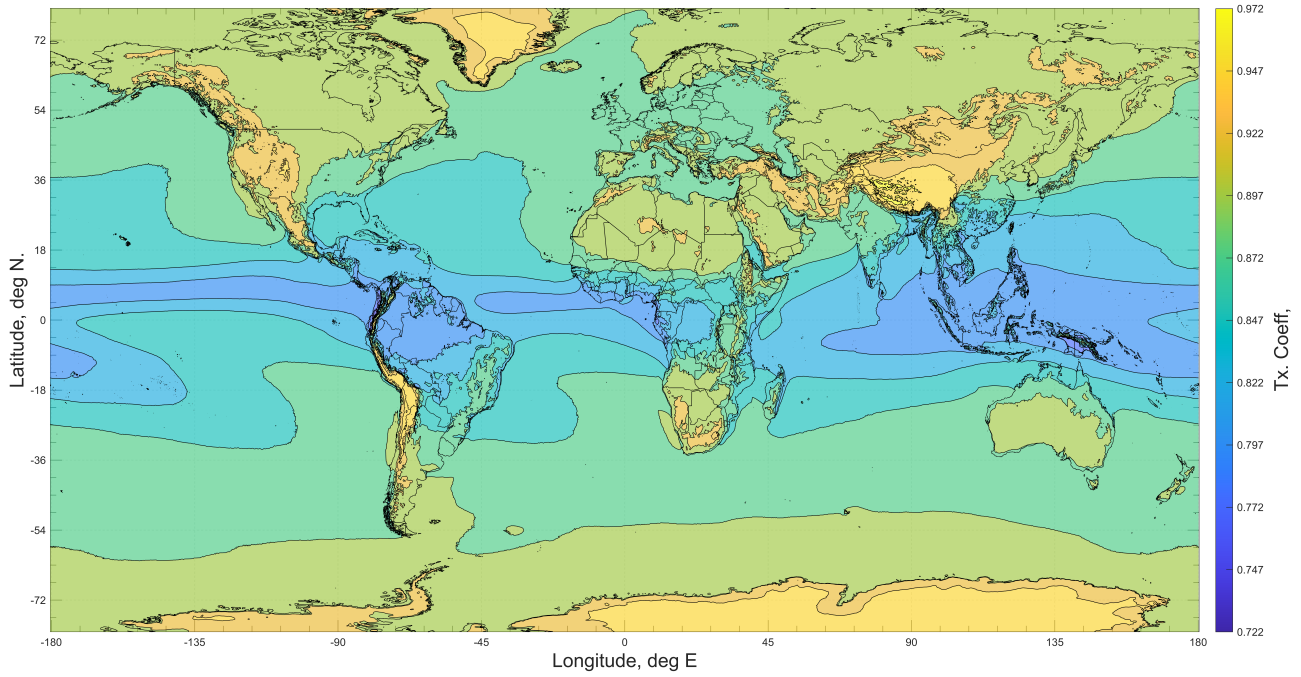

Figure 2. Zenith transmission coefficient β_0 computed at 42 GHz. Clear sky, p%=50; median value: 0.89; inter-quartile range: 0.04.
Source: Author.

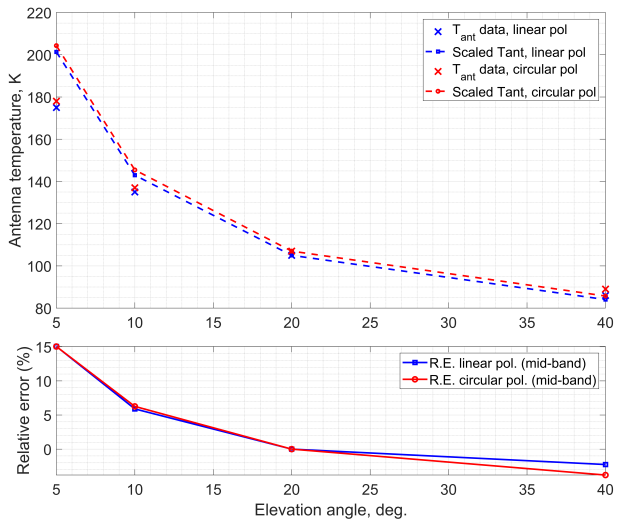

Figure 3. Evaluation of the error performance of Eq. (15) in scaling the antenna noise temperature of a 1.2 m Ka-band terminal from the known value at a 20° elevation. The median value of β_0 is used at the mid-band frequencies of 20.25 (0.9385) and 20.3 GHz (0.9374).
Source: Author

of the RF aperture, this simplified model may not be accurate even at elevation angles close to 20°, as the antennas may still exhibit a non-negligible gain towards the ground. For antennas mounted on airplanes or ships, the structure's contribution to antenna noise also affects the magnitude of the ground noise contribution and impacts the validity of the model.

b. **Limitations arising from the cosecant scaling assumption.** The cosecant scaling assumption (*i.e.*, the use of $\frac{1}{sin(\theta)}$ to scale attenuation) is present in the ITU-R statistical models for predicting both gas and cloud attenuation [16, 17]. Cosecant scaling has shown increased prediction errors when used with angles below 20° for cloud attenuation [21] and below 5° for gas attenuation, where [16] recommends a ray-tracing procedure. Therefore, and especially for frequencies in the 100 GHz range, the applicability of the method for scaling under clear-sky conditions below 20° is limited.

Developing a method to compute the increases in Earth station noise temperature in the presence of rain

General formulation for the changes in system noise temperature due to the presence of rain in the space-to-Earth path

The analysis of the increase in noise temperature due to atmospheric attenuation (i.e., when the link experiences rain) increases in relevance commensurately with an increase of frequency of operation. As explained in previous sections, understanding the increase in noise temperature is necessary to account for the total degradation experienced by the link, which is composed of the attenuation in the path and the increase in system noise temperature. Recall the expression for total system downlink noise degradation (DND) [22] :

$$DND = A + 10 \cdot \log_{10}\left(\frac{T_{\text{sys, faded}}}{T_{\text{sys, C.W}}}\right), \tag{16}$$

with A (in dB) being the total attenuation experienced by the link (*i.e.*, the sum of rain, gas, clouds, and tropospheric scintillation). If the only figure available to the designer is a total system noise temperature under clear-sky conditions, the application of the total system degradation expression

is not immediately possible. Thus, the issue lies in determining $T_{\text{sys, faded}}$ when the reference conditions for the clear weather computations are not explicitly known. It is for this situation that an expression to quantify the increase in system temperature with respect to the known clear-sky values becomes useful, as will be further explained in this section.

Note that the equivalent system temperature under fade follows the model in Eq. (3):

$$T_{\text{sys, faded}}(l_{\text{atm, faded}}) = \frac{T_{\text{ant, faded}}(l_{\text{atm, faded}})}{l_{\text{f}}} + \ldots \\ T_{\text{f, p}'} \cdot (1 - l_{\text{f}}^{-1}) + T_{\text{LNB}} \tag{17}$$

with

- $T_{\text{ant, faded}}$ (K) being the antenna noise temperature in the presence of tropospheric fade (clouds, rain, and gases, denoted as $l_{\text{atm, faded}}$)
- $T_{\text{f, p}'}$ (K) being the feeding network's physical temperature during a rain event

The objective of this section is to develop the expression for ΔT_{sys}, *i.e.*, the difference between the system noise temperatures in clear sky and under fade. Considering that the presence of fade increases the noise temperature, for the ΔT value to be positive by definition, the expression must be as follows:

$$\Delta T_{\text{sys}} = T_{\text{sys, faded}}(l_{\text{atm,faded}}) - T_{\text{sys,C.W}}(l_{\text{atm, C.W.}}) \tag{18}$$

In Eqs. (17) and (18), the dependence of ΔT_{sys} on atmospheric loss becomes clear. In the discussion that follows, and to simplify the presentation of the equations, the explicit dependence of the system temperature on the atmospheric loss (l_{atm}) will be removed, but the relevant sub-indices will be retained to refer to each condition (clear weather or degraded/rainy weather).

For a given location and elevation angle, expanding Eq. (18) using (3) and (17) yields the following, noting that T_{LNB} is the same in both equations:

$$\Delta T_{\text{sys}} = \frac{1}{l_f} \cdot (T_{\text{ant, faded}} - T_{\text{ant, C.W.}}) + (1 - l_f^{-1}) \cdot (T_{\text{f,p}'} - T_{\text{f,p}}) \tag{19}$$

Denoting $(T_{\text{ant, faded}} - T_{\text{ant, C.W.}})$ as ΔT_{ant}, the Earth station system noise temperature increase is expressed as follows:

$$\Delta T_{\text{sys}} = \frac{1}{l_f} \cdot \Delta T_{\text{ANT}} + \delta T_{\text{f,p}} \cdot (1 - \frac{1}{l_f}) \tag{20}$$

The term $\delta T_{\text{f,p}} = T_{\text{f, p}'} - T_{\text{f, p}})$ represents the change in the physical temperature of the feeding network during the rain event.

Eq. (19) can be reduced to $\Delta T_{ant} = T_{\text{ant, faded}} - T_{\text{ant, C.W.}}$ under two scenarios:

a. When the losses between the antenna flange and the LNB are small: as the losses (in linear units) tend to 1, their contribution tends to zero. This is the case with terminals such as video or broadband direct-to-home (DTH) terminals.

b. When the change in the physical temperatures $\delta T_{\text{f,p}}$ is very small: as physical temperatures, $T_{f,p}$ and $T_{f,p'}$ are expected to differ during rain events where the surface temperature is slightly lower and water contributes to cooling the hardware. However, the magnitude of the change may not be greater than a few °C. As the change tends to zero, the noise increase also tends to zero.

T_{ant} for clear sky and faded conditions

The next step in constructing our model goal is to expand upon $T_{\text{ant,faded}} - T_{\text{ant, C.W.}}$.

As noted, during a rain event, the antenna temperature changes due to an increase in the atmospheric attenuation $l_{\text{atm,faded}}$ and by the changes in the physical temperature of the radome $T_{\text{RAD,p}'}$. The atmosphere's contribution to the antenna noise temperature is determined using the atmosphere's mean radiating temperature, *i.e.*, $\text{T}_{\text{MR}'}$.

$$T_{\text{ant, faded}} = \frac{T_{Bo}}{l_{\text{atm, faded}} \cdot l_{\text{RAD}}} + \frac{\text{T}_{\text{MR}'}}{l_{\text{RAD}}} \cdot (1 - l_{\text{atm, faded}}^{-1}) \ldots \\ + \frac{T_{\text{gnd}}}{l_{\text{RAD}}} + T_{\text{RAD, p}'} \cdot (1 - l_{\text{RAD}}^{-1}) \tag{21}$$

An important assumption in Eqs. (6) and (21) is that the attenuation in the atmosphere does not affect the ground's contribution to the antenna noise. As previously mentioned, given that this contribution includes a component of reflected emissions from the sky, it will change in the presence of rain due to the increase in emissions from the atmosphere and the change in ground conductivity. Furthermore, and depending on the materials used to construct the radome, an additional attenuation $l_{\text{radome–wetting}}$ may need to be considered and folded into the l_{RAD} term, stemming from the potential buildup of a water layer on the radome, which causes signal attenuation. Coating radomes with hydrophobic paint can help minimize the water build-up and reduce the additional attenuation.

ΔT_{ant} can now be determined by subtracting Eqs. (21) and (6). After grouping the terms associated to cosmic background, atmosphere, ground and radome, the following expression is obtained:

$$\Delta T_{\text{ant}} = \left(\frac{T_{\text{Bo}}}{l_{\text{atm, faded}} \cdot l_{\text{RAD}}} - \frac{T_{\text{Bo}}}{l_{\text{atm, C.W.}} \cdot l_{\text{RAD}}} \right) + \ldots \\ \left(\frac{\text{T}_{\text{MR}'}}{l_{\text{RAD}}} \cdot (1 - l_{\text{atm, faded}}^{-1}) - \frac{\text{T}_{\text{MR}}}{l_{\text{RAD}}} \cdot (1 - l_{\text{atm, C.W.}}^{-1}) \right) + \ldots \\ \left(\frac{T_{\text{gnd}}}{l_{\text{RAD}}} - \frac{T_{\text{gnd}}}{l_{\text{RAD}}} \right) + \ldots \\ \left(T_{\text{RAD, p}'} \cdot (1 - l_{\text{RAD}}^{-1}) - T_{\text{RAD, p}} \cdot (1 - l_{\text{RAD}}^{-1}) \right), \tag{22}$$

which can be rewritten as follows (noting that the ground contribution term cancels out):

$$\Delta T_{\text{ant}} = \left[\frac{T_{\text{Bo}}}{l_{\text{RAD}}} \cdot \left(\frac{1}{l_{\text{atm, faded}}} - \frac{1}{l_{\text{atm, C.W.}}}\right)\right] + \ldots \left[\frac{1}{l_{RAD}} \cdot \left(\delta T_{MR} + \left(\frac{T_{MR}}{l_{\text{atm, C.W.}}} - \frac{T_{MR'}}{l_{\text{atm, faded}}}\right)\right)\right] + \ldots \left[\delta T_{\text{RAD, p}} \cdot \left(1 - \frac{1}{l_{\text{RAD}}}\right)\right], \tag{23}$$

with

- δT_{MR} being the difference in the mean radiating temperature, *i.e.*, $(T_{\text{MR}'} - T_{\text{MR}})$
- δT_{RAD} being the difference in the physical temperature of the radome in clear sky and during rain, *i.e.*, $T_{\text{RAD, p}'} - T_{\text{RAD, p}}$

Simplifying ΔT_{ant}

Eq. (23) contains three contributors (separated by brackets for convenience):

- A contribution due to the background radiation, T_{Bo}
- A contribution from the atmosphere
- A contribution from the radome

By studying each contributor, a simplification to the ΔT_{ant} equation can be proposed.

Simplifying the atmospheric loss term: variation of T_{MR}.

The atmospheric contribution term in Eq. (23) includes the variation in the mean radiating temperature with respect to its clear-sky value (δT_{MR}). Therefore, it is useful to explore the dependence of T_{MR} on parameters such as the link's operating frequency and the surface temperature.

Variation of T_{MR} with frequency. Studies carried out by the European Space Agency [23] indicate a weak dependence of T_{MR} on frequency: at a fixed location, in the range of 5-50 GHz, the variation was between 2 and 15 K. An average location-specific value could be used without sacrificing precision, and the study provides a grid of frequency-averaged clear-sky T_{MR} values for locations on the surface of the Earth with a resolution of 0.75°. For the cited study, the median value of the clear-sky T_{MR} is 269.3 K, averaged over frequencies and computed across the world grid, excluding latitudes above ±80°. The minimum and maximum values are 241.8 K and 284.2 K, respectively.

Variation of T_{MR} with atmospheric temperature. With respect to the atmospheric temperature, for a fixed geographical location and frequency, the values of T_{MR} under clear-sky and rain conditions are strictly different, but they may not differ by much. The ITU-R [24] indicates that T_{MR} may be assumed equal to the ambient temperature for frequencies up to 40 GHz. To understand the magnitude of the difference in the mean radiating temperatures, one can use linear models to compute T_{MR} based on the surface temperature [25, 26], or link the mean radiating temperature to the conditions of the propagation channel [9], which yields a linear model to compute an effective T_{MR} based on the cumulative distribution of the path attenuation $P(A)$ as $T_{MR} \approx 255 + 25 \cdot P(A)$, with $P(A)$ being the cumulative probability that an attenuation value is exceeded.

Even if T_{MR} varies under instantaneous weather conditions, ITU-R Recommendation P.618-13 [26] recommends using a value of 275 K in the absence of local data for both clear and rainy weather. This value was further clarified in [27]. Therefore, the assumption of a constant value for T_{MR} as a rough approximation is not without precedent.

Taking advantage of the above, the term δT_{MR} can be equal to zero, and the atmosphere-related term in Eq. (23) can be reduced as follows:

$$\frac{1}{l_{\text{RAD}}} \cdot \left[\delta T_{\text{MR}} + \left(\frac{T_{\text{MR}}}{l_{\text{atm, C.W.}}} - \frac{T_{\text{MR}'}}{l_{\text{atm, faded}}}\right)\right] \approx \frac{T_{\text{MR}}}{l_{\text{RAD}}} \cdot \left(\frac{1}{l_{\text{atm, C.W.}}} - \frac{1}{l_{\text{atm, faded}}}\right) \tag{24}$$

Reducing the contribution of the radome loss.

By observing the term associated with the radome loss, one may note the presence of a similar factor representing the difference in the radome's physical temperatures under clear weather and during rain.

$$\delta \text{T}_{\text{RAD,p}} \cdot \left(1 - \frac{1}{\text{l}_{\text{RAD}}}\right) \tag{25}$$

It should be noted that the magnitude of the change in the physical temperature of the radome may be different to that of the feeding network. The change in temperature depends, for example, on the characteristics of the materials used to build the radome, as well as on its type. Moreover, it may be affected by the changes in the EIRP of the Earth station, in cases where uplink power control (UPC) is used with high power amplifiers.

Notwithstanding the above, the contribution of the radome loss can be eliminated from Eq. (23) if the change in the physical temperature is very small (making $\delta \text{T}_{\text{RAD,p}} \approx 0$).

Final expressions for the change in the Earth station's system temperature in the presence of rain in the space-to-Earth path

Finally, we can propose some variations of the model for ΔT, considering the above-presented avenues for simplification.

Expression assuming $\delta T_{\text{MR}} \approx 0$ and identical changes in physical temperature. Starting from Eq. (23), assuming that T_{MR} is the same in clear weather and during fade events and that the changes in the physical temperatures $\delta T_{\text{RAD, p}}$ and $\delta T_{\text{f, p}}$ are identical and equal to δT_p, substituting into Eq. (20) yields the following:

$$\Delta T_{\text{ant}} = \frac{1}{l_f \cdot l_{\text{RAD}}} \cdot \left[T_{\text{Bo}} \cdot \left(\frac{1}{l_{\text{atm, faded}}} - \frac{1}{l_{\text{atm, C.W}}} \right) \cdots + T_{\text{MR}} \cdot \left(\frac{1}{l_{\text{atm, C.W.}}} - \frac{1}{l_{\text{atm, faded}}} \right) \right] + \delta T_p \cdot \left(1 - \frac{1}{l_f \cdot l_{\text{RAD}}} \right) \tag{26}$$

Expression assuming δT_{MR}, $\delta T_{\text{RAD, p}}$, and $\delta T_{\text{f, p}} \approx 0$ and negligible changes in physical temperature. By taking Eqs. (23) and (20) and eliminating the terms related to changes in physical temperature, *i.e.*, $\delta T_{\text{RAD, p}}$ and $\delta T_{f,\,p}$ |since this scenario entails a value of zero|, we obtain

$$\Delta T_{\text{ant}} = \frac{1}{l_f \cdot l_{RAD}} \cdot \left[T_{Bo} \cdot \left(\frac{1}{l_{\text{atm, faded}}} - \frac{1}{l_{\text{atm, C.W.}}} \right) \cdots + T_{\text{MR}} \cdot \left(\frac{1}{l_{\text{atm, C.W.}}} - \frac{1}{l_{\text{atm, faded}}} \right) \right]. \tag{27}$$

The changes in physical temperature between the clear-sky and rainy conditions can be ignored for cases where the Earth station hardware is in a controlled space, as is the case with large Earth stations featuring refrigerated LNA systems and installed in climate-controlled enclosures.

Expression assuming $\delta T_{\text{MR}} \approx 0$ and l_f, $l_{\text{RAD}} = 0$. The simplest model for ΔT_{sys} |valid for very compact receive chains or fully integrated systems without a radome and minimal passive network losses| assumes a constant value of T_{MR} and equal physical temperatures:

$$\Delta T_{\text{ant}} = T_{\text{Bo}} \cdot \left(\frac{1}{l_{\text{atm, faded}}} - \frac{1}{l_{\text{atm, C.W.}}} \right) \cdots + T_{\text{MR}} \cdot \left(\frac{1}{l_{\text{atm, C.W.}}} - \frac{1}{l_{\text{atm, faded}}} \right), \tag{28}$$

which indicates that the only changes are due to increased antenna noise temperature under fade.

Applications

This section illustrates how the proposed models can be applied to system engineering situations in the satellite communications industry. The examples in this section reflect practical cases in systems and spectrum engineering.

Use case 1: adjusting the clear-sky system temperature from a known value at a reference elevation angle.

Consider a Ka-band (18.1 to 20.2 GHz) communications scenario using a 65 cm reflector-based maritime user terminal [28] and an E-band 1.8 m gateway station [29], whose service performance needs to be evaluated in a variety of clear sky satellite link scenarios with different elevation angles. This scenario may occur, for instance, in solution optimization problems involving a roaming terminal and in multi-orbit operations using a constellation of GEO and non-GEO satellites.

In this scenario, the information at hand is the following:

- For the user terminal, the G/T is 15.5 dB/K at 10°, and the boresight gain is 40.2 dBi at a reference frequency of 19 GHz, as reported by the product datasheet [28].
- For the E-band gateway, the antenna gain is 60 dBi at a reference frequency of 73.5 GHz.

The inputs and associated assumptions are summarized in Table 2.

Considering that this scenario involves multiple link combinations and different elevation angles, the scaling equation provided in Eq. (15) is useful to determine the system noise temperature at an angle θ, which is required for obtaining the G/T and include it in the solutions engineering and optimization process. The resulting curve for the system noise temperature *vs.* the elevation angle is presented in Fig. 4.

Table 2. Example inputs for constructing an Earth station noise temperature *vs.* elevation angle curve. No radome or feeding network loss is assumed. Additional assumptions for the gateway terminal include the LNB temperature and the gateway's elevation angle.

Parameter	User terminal	Gateway	Units
Frequency	19.0	73.5	GHz
Ant. diameter	0.65	1.8	m
Ant. gain	40.2	60	dBi
Elev. angle	10	90	degrees
G/T	15.5	-	dB/K
T_{LNB}	-	360	K
Median value of β_0	0.9587	0.7483	-
T_{SYS}	295.12	448.7	K

Source: Author

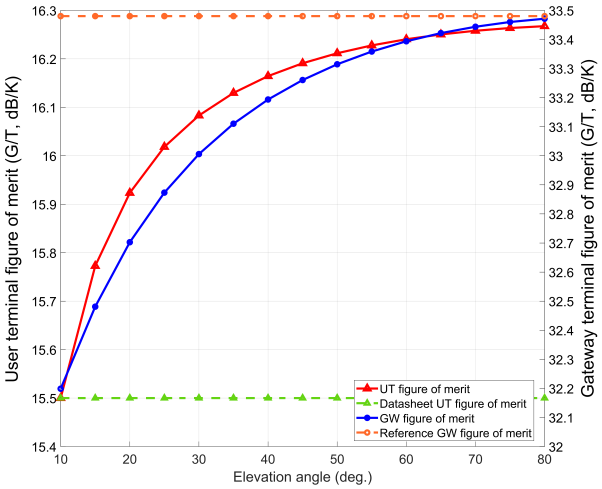

Figure 4. G/T *vs.* elevation angle curve developed using the scaling model for the user and gateway terminals
Source: Author

The benefits of the model are apparent: when analyzing the 65 cm user terminal, there is an improvement of the G/T with increased elevation angles (up to 0.7 dB at 70°) that would not otherwise have been considered. Conversely, the gateway's G/T degrades from the reference zenith value. Ignoring this change at higher frequencies (*e.g.*, the E-band at 70 GHz) –especially in tropical regions, where the water vapor content in the atmosphere is more notable– leads

to sub-optimal solutions, such as overestimations of power consumption and bandwidth allocation.

Use case 2: adjusting the value of the clear-sky system temperature when the reference elevation angle is not known.

This example uses the information in [15] for the coexistence of GEO and non-GEO systems in the Q/V band. As discussed in a previous section, the 45 and 60 cm Earth stations' part of the reference links is characterized by a single noise temperature of 340 K, regardless of the elevation angle. With this value, the G/Ts of the user terminal are 18.5 and 21 dB/K for 45 and 60 cm, respectively. This scenario analyzes the links at two locations: one tropical (Cali, Colombia) and one temperate (Rome, Italy).

To apply Eq. (15), it is necessary to establish the reference elevation angle. A conservative assumption is to apply the provided system temperature of 340 K to the zenith angle. In doing so, the noise temperature can only increase as the elevation angle decreases from the zenith. The G/T for each location |computed for the 20 and 55° elevation angles indicated in [15]| and the corresponding increase in G/T (ΔG/T) are presented in Table 3 for the temperate location and in Table 4 for the tropical one. Notably, it is in tropical locations where the largest change in system temperature is observed (0.8 dB), given the increased contribution of clear-sky cloud and water vapor attenuation to the antenna noise.

Table 3. G/T of user terminals (UT) for links in ITU-R Resolution 770. Frequency: 42.5 GHz. Reference G/T: 18.5 dB/K for 45 cm and 21 dB/K for 60 cm. $\theta_{\text{ref}} = 90$). Temperate location: Rome (IT). $\beta o = 0.8828$. $T_{\text{MR}} = 275$ K.

UT size (m)	Gain	Elev. (deg)	T_{SYS}	G/T	ΔG/T
0.45	43.2	20	378.9	17.9	0.61
0.45	43.2	55	344.8	18.4	0.08
0.6	45.7	20	378.9	20.4	0.61
0.6	45.7	55	344.8	20.9	0.08

Source: Author

Table 4. G/T of user terminals for links in ITU-R Resolution no. 770. Frequency: 42.5 GHz. Reference G/T: 18.5 dB/K for 45 cm and 21 dB/K for 60 cm. $\theta_{\text{ref}} = 90$. Tropical location: Cali (CO). $\beta o = 0.7779$. $T_{\text{MR}} = 275$ K.

UT size (m)	Gain	Elev. (deg)	T_{SYS}	G/T	ΔG/T
0.45	43.2	20	378.9	17.5	0.94
0.45	43.2	55	344.8	18.3	0.14
0.6	45.7	20	378.9	20.4	0.94
0.6	45.7	55	344.8	20.8	0.14

Source: Author

Conclusions

The main objective of this paper was to provide equations that incorporate variations in Earth station noise temperature arising from the conditions of the satellite channel. The two contributions of the paper, Eqs. (15) and (20), are a product of the development of an expression for ΔT_{SYS} based on the reference receive chain noise model for clear-sky conditions presented in Eq. (3). Throughout the derivation steps, we examined the impact of the atmospheric transmission coefficient and the atmosphere's mean radiating temperature, two key parameters in the estimation of the noise contribution of the atmosphere. In addition, some avenues to simplify the methods were formulated, yielding useful expressions for situations wherein the Earth station noise temperature is provided with no additional information regarding the components of the receive chain or the reference elevation angle associated to the equivalent system temperature, as is often the case with spectrum-oriented inter-system sharing analyses.

As the system's operating frequency increases (*e.g.*, in systems using the V, E, and W bands), this assumption of constant temperature becomes less adequate. As shown in the numerical examples, the use of the proposed methods is beneficial since it allows capturing changes in G/T that would otherwise be ignored. The proposed equations can then be integrated into system capacity analyses for non-GEO constellations, which traditionally adhere to the constant clear-sky noise temperature.

Considering the objective of providing a straightforward approach to aid system design when detailed user terminal data are not available, potential avenues for future work could include antenna noise temperature calculations using reference gain envelopes such as those in ITU-R Recommendation S.580, or functional pattern approximations like Bessel functions as proxies for the actual user terminal radiation patterns, as well as the use of a more adequate attenuation scaling approach for the cloud contributions at very high frequencies.

Acknowledgments

The author would like to thank Dr. C. Lacoste for his help with LaTeX formatting and proofreading, as well as to Dr. J. Krause, Dr. Domingo Pimienta, and Professors L. Luini and J. M. Riera for their valuable contributions to the clarity of this document.

Author contributions

L. E. conceived the idea, conducted the literature search, developed the methods, and wrote the manuscript.

Conflicts of interest

The author declares no conflicts of interest.

References

[1] G. Maral, M. Bousquet, and Z. Sun, *Satellite Communications Systems*, 6th ed. Hoboken, NJ: John Wiley and Sons, Ltd, 2020.

[2] J. Allnut and T. Pratt, *Satellite Communications*, 3rd ed. Hoboken, NJ: John Wiley and Sons, Ltd, 2020.

[3] International Telecommunications Union, Radiocommunication Sector (ITU-R), *Resolution 770 (WRC-19). Application of Article 22 of the Radio Regulations to the protection of geostationary fixed-satellite service and broadcasting-satellite service networks from non-geostationary fixed-satellite service systems in the frequency bands 37.5-39.5 GHz, 39.5-42.5 GHz, 47.2-50.2 GHz and 50.4-51.4 GHz,*

Resolution 770 (WRC-19)., Geneva, CH, 2019. [Online]. Available: https://www.itu.int/dms_pub/itu-r/oth/0C/0A/R0C0A00000F00166PDFE.pdf

[4] International Telecommunication Union, Radiocommunication Bureau, "Report of the Conference Preparatory Meeting (CPM) on technical, operational and regulatory/procedural matters to be considered by the World Radiocommunication Conference 2023 (WRC-23)," International Telecommunications Union (ITU), Geneva, CH, 2023. [Online]. Available: https://www.itu.int/dms_pub/itu-r/md/19/cpm23.2/r/R19-CPM23.2-R-0001!!PDF-E.pdf

[5] International Telecommunications Union, Radiocommunication Sector (ITU-R), *World Radiocommunication Conference 2023 (WRC-23), Final Acts*, 2023. [Online]. Available: https://www.itu.int/dms_pub/itu-r/opb/act/R-ACT-WRC.16-2024-PDF-E.pdf

[6] Jet Propulsion Laboratory, JPL. DESCANSO. Deep Space Communications and Navigation Center of Excellence [Online]. Available: https://descanso.jpl.nasa.gov/. [Accessed: 29 June, 2024].

[7] T. Otoshi, *Noise Temperature Theory and Applications for Deep Space Communications Antenna Systems*. Norwood MA: Artech house, 2009.

[8] ——, "Calculation of Antenna System Noise Temperatures at Different Ports Revisited," *Interplanetary Network Progress Report, INPR.*, vol. 42, no. 150, pp. 1–18, 2002. [Online]. Available: https://ipnpr.jpl.nasa.gov/progress_report/42-150/150F.pdf

[9] NASA Jet Propulsion Laboratory, *Telecommunications Link Design Handbook*, 2024. [Online]. Available: https://deepspace.jpl.nasa.gov/dsndocs/810-005/

[10] Cortes-Medellin, G., "SKA memo 95. Antenna Noise Temperature Calculation," 2007. [Online]. Available: www.skatelescope.org

[11] Next Generation Very Large Array (ngVLA). [Online]. Available: https://ngvla.nrao.edu/. [Accessed: 29 June, 2024].

[12] ——. Technical Memos (Antenna) [online]. https://ngvla.nrao.edu/page/memos#tech-memo-ant. [Accessed: 29 June, 2024].

[13] B. Butler, W. Grammer, and R. Lehmensiek, "ngVLA memo 96. ngVLA Antenna Noise Temperature Calculation." 2021. [Online]. Available: https://library.nrao.edu/public/memos/ngvla/NGVLA_96.pdf

[14] D. I. L. de Villiers and R. Lehmensiek, "Rapid Calculation of Antenna Noise Temperature in Offset Gregorian Reflector Systems," *IEEE Trans. Antennas Propag.*, vol. 63, no. 4, pp. 1564–1571, 2015.

[15] *Recommendation S.2157. Procedures for the evaluation of interference from any non-geostationary-satellite system into a global set of the generic geostationary-satellite reference links in the frequency bands 37.5-39.5 GHz (space-to-Earth), 39.5-42.5 GHz (space-to-Earth), 47.2-50.2 GHz (Earth-to-space) and 50.4-51.4 GHz (Earth-to-space).*, International Telecommunications Union, Radiocommunication Sector (ITU-R). Geneva, CH, 2023. [Online]. Available: https://www.itu.int/rec/R-REC-S.2157/en

[16] *Recommendation P.676-13. Attenuation by atmospheric gases and related effects*, International Telecommunications Union, Radiocommunication Sector (ITU-R). Geneva, CH, 2022. [Online]. Available: https://www.itu.int/rec/R-REC-P.676/en

[17] *Recommendation P.840-8. Attenuation due to clouds and fog*, International Telecommunications Union, Radiocommunication Sector (ITU-R) Geneva, CH, 2019. [Online]. Available: https://www.itu.int/rec/R-REC-P.840/en

[18] *Recommendation S.733. Determination of the G/T ratio for Earth stations operating in the fixed-satellite service*, International Telecommunications Union, Radiocommunication Sector (ITU-R) Geneva, CH, 2000. [Online]. Available: https://www.itu.int/rec/R-REC-S.733/en

[19] *Recommendation P.835. Reference standard atmospheres.*, International Telecommunications Union, Radiocommunication Sector (ITU-R) Geneva, CH, 2017. [Online]. Available: https://www.itu.int/rec/R-REC-P.835/en

[20] CPII-Satcom and antenna technologies division. Vsat antennas tx/rx [Online]. Available: https://www.cpii.com/product.cfm/15/127/706. [Accessed: 15 January, 2025].

[21] L. Luini and C. Capsoni, "Scaling cloud attenuation statistics with link elevation in earth-space applications," *IEEE Trans. Antennas Propag.*, vol. 64, no. 3, pp. 1089–1095, 2016.

[22] J. Allnut, *Satellite-to-Ground radiowave propagation*, 2nd ed. Stevenage, UK: The Institution of Engineering and Technology (IET), 2011.

[23] France, Italy, and European Space Agency (ESA), "ITU-R WP3M information document 235. Improvement of the model of sky brightness temperature in clear sky conditions from ERA Interim profile and surface data," 2015. [Online]. Available: https://www.itu.int/md/R12-WP3M-C-0235

[24] International Telecommunications Union, Radiocommunication Sector (ITU-R), *Handbook on Radiometeorology*, ITU-R SG3 Handbook, 2013. [Online]. Available: https://www.itu.int/dms_pub/itu-r/opb/hdb/R-HDB-26-2013-OAS-PDF-E.pdf

[25] A. Alyosef, D. Cimini, L. Luini, C. Riva, F. Marzano, M. Biscarini, L. Milani, A. Martellucci, S. Gentile, S. Nilo, F. D. Paola, A. Alkhateeb, and F. Romano, "Improving atmospheric path attenuation estimates for radio propagation applications by microwave radiometric profiling," *Atmos. Meas. Tech.*, vol. 14, no. 4, pp. 2737–2748, 2021.

[26] *Recommendation P.618-13. Propagation data and prediction methods required for the design of Earth- space telecommunication systems*, International Telecommunications Union, Radiocommunication Sector (ITU-R) Std., 2017. [Online]. Available: https://www.itu.int/rec/R-REC-P.618/en

[27] V. Mattioli, F. S. Marzano, N. Pierdicca, C. Capsoni, and A. Martellucci, "Modeling and predicting sky-noise temperature of clear, cloudy, and rainy atmosphere from X- to W-band," *IEEE Trans. Antennas Propag.*, vol. 61, no. 7, pp. 3859–3868, 2013.

[28] Intellian Technologies Inc. v45C 45cm Compact & Light Ku-band VSAT antenna [Online]. Available: https://www.intelliantech.com/en/products/compact-maritime-vsat/v45c/. [Accessed: 08 August, 2024].

[29] SpaceX Services Inc., "Application for Earth Station authorizations. FCC SAT-LIC-2023-05250-1111," 2023. [Online]. Available: https://fcc.report/IBFS/SES-LIC-20230525-01110